Constraint Effect in Fracture – What Is It?

Yuh J. Chao[1] and Poh-Sang Lam[2]
[1]University of South Carolina, Columbia, SC 29208, USA, E-mail:chao@sc.edu
[2]Savannah River National Laboratory, Aiken, SC 29808, USA

Abstract

The meaning of the phrase "*constraint effect in fracture*" has changed in the past two decades from "contained plasticity" to a broader description of "dependence of fracture toughness value on geometry of test specimen or structure." This paper will first elucidate the fundamental mechanics reasons for the apparent "constraint effects in fracture", followed by outlining a straightforward approach to overcoming this problem in both brittle (elastic) and ductile (elastic-plastic) fracture. It is concluded by discussing the major difference in constraint effect on fracture event in elastic and elastic-plastic materials.

1. The root cause of "Constraint Effect in Fracture" in nonlinear materials

Although fracture mechanics has been around for over 50 years, the subject of "constraint effect in fracture" is relatively recent, which only started in early 1990's. There were two timely symposia dedicated to the constraint effect in fracture by ASTM in 1993 [1] and 1994 [2].

In early years, the term "contained plasticity" referred to the plasticity aspects of deeply cracked, bending specimens where the plasticity at high level of load is contained in a small region near the crack tip. On the other hand, CCP (center cracked panel) and SENT (single edge notched tension) specimens have plasticity spread out extensively to the far field when the applied load level is high. This is best seen with the markedly different slip-line fields in these specimens. Inspired by these different slip-line fields, McClintock had proclaimed the possible 'non-uniqueness' of crack tip fields in low hardening materials [3]. Specimens that possess "contained plasticity" are nowadays referred to as "high constraint" geometry and the opposite is then "low constraint." It is important to keep in mind that "high" or "low" is relative.

In 1968, Hutchinson [4,5] and Rice and Rosengren [6] developed the crack tip stress field for power-law nonlinear materials. The so-called HRR solution assumes small strain theory, that is, large strains and large geometry change such as blunting are not considered. In addition, the analysis keeps only the first term in the asymptotic series expansion. As such it is valid only as r approaches zero with the origin of the coordinate system set at the crack tip.

Figure 1 shows the opening stress in front of a crack plotted as a function of non-dimensional distance $r/(J/\sigma_o)$, where J is the applied J-integral [7], and σ_o is the yield stress of the material. In Figure 1, curve A represents the HRR solution; curve B is the stress obtained from a small strain finite element (FE) analysis; and curve C is the stress determined from finite strain FE analysis. In reality, the stress at the close vicinity of the crack tip is affected by three-dimensional effects, large deformations, and microstructure fracture processes, etc. The size of this fracture process zone is often believed to coincide with the size of the region where finite strain effects are significant, that is, close to curve C. In the limit as r approaches zero, curve B approaches curve A asymptotically. As r increases these two solutions gradually deviate from each other since the HRR solution is only valid asymptotically. On the other hand, curves B and C will coincide beyond the region where the large strain effect is significant.

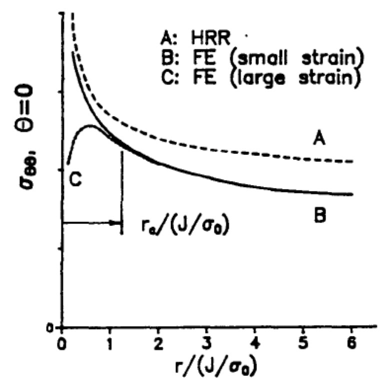

Figure 1 Crack tip stress fields

Figure 2 shows the crack tip opening stress plotted similar to Figure 1, but for two extreme cases: one for a high constraint specimen geometry and the other a low constraint specimen. High constraint geometry includes bending or/and deeply cracked specimen. For low constraint specimen geometry, it includes shallow crack or/and under tension. Figure 2b shows that in some cases of high constraint geometry, the stress distribution is close to the HRR even as the load becomes high. However, in the low constraint geometry (Figure 2a), the stresses gradually deviate from HRR solution as the load increases. In other words, under low loading or small scale yielding (SSY), the HRR solution could be used to characterize the stress fields. Under higher load or large scale yielding (LSY), the HRR solution may not be sufficient to characterize the crack tip stress field, especially for low constraint specimens. Since fracture of solids is controlled by stress, strain or a combination of the two (e.g., strain energy), it may be stated that under SSY a single parameter (e.g. J from HRR solution) could be used to determine the fracture event. On the other hand, J alone may be inadequate to characterize fracture under LSY conditions or for low constraint specimen/structures.

Note that in Figure 2, all curves converge to HRR as r approaches zero because HRR solution is asymptotically correct (under the assumed conditions). Difference can be seen between the curves for *any* finite values of r. In a fracture process zone model the fracture event is controlled by the stress/strain at *a finite* r ahead of the crack tip, as shown in Figure 1 (denoted as r_c). In such a case, a higher failure load for the low constraint specimen/structure would be predicted at the critical distance (r_c) if the *J*-dominated stress solution (i.e. HRR) is used. As seen in the fracture testing, higher fracture toughness is generally obtained from a low constraint, shallow crack configuration when compared to the standard, deeply cracked specimen.

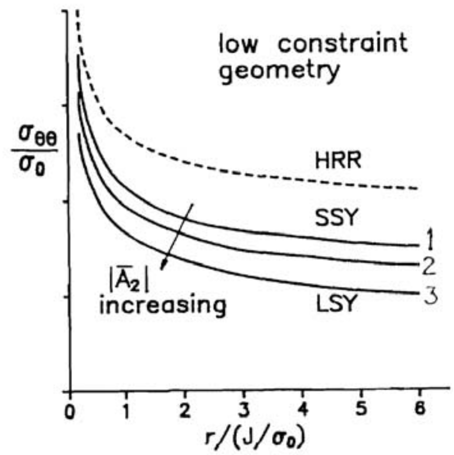

Figure 2a Stress ahead of a crack tip in low constraint specimen geometry

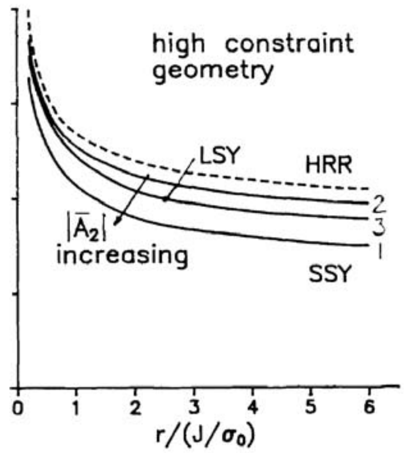

Figure 2b Stress ahead of a crack tip in high constraint specimen geometry

The above discussion demonstrates the need for developing theories of the so called "constraint in fracture" in elastic-plastic, non-linear materials, in which the stress distribution at a *finite distance* from the crack tip cannot be accurately characterized by the classical HRR solution, as shown in Figure 2. This phenomenon is especially true under LSY conditions and low constraint geometry which occur in many ductile metals such as mild steels.

2. Remedy

As the root cause of the "constraint effect" is the deviation of the stress from HRR solution at a *finite* distance from the crack tip, the premise of "asymptotic" implies that this stress could be described with better accuracy if higher order terms, in addition to the first term as in HRR, are considered in the series expansion. Based on this conjecture, the author and his colleagues have developed mathematical asymptotic mechanics solutions near a crack tip [8-10], which includes several higher order terms. The mathematical formulation and assumptions are similar to Hutchinson [4,5] and Rice and Rosengreen [6]; but the solution procedure is much more elaborated because each of the higher order terms (in terms of *r* to certain power) has many possibilities and each option must be carefully examined and analyzed.

Although several higher order terms can be obtained, it was shown that the stress, strain and displacement fields can be well characterized by the analytical solution with only three terms, up to a large portion of the plastic zone for a variety of fracture testing specimens for $n \geq 3$, where n is the strain hardening exponent in the Ramberg-Osgood stress-strain law. Referring to Figure 1, the higher-order analytical solution coincides with curve B from the crack tip to a distance well beyond $r/(J/\sigma_0) = 5$ which is several times of the crack tip opening displacement. These three terms, as shown in Eq. 1, are controlled by only two, not three, parameters (i.e., J and A_2) under Mode I plane strain conditions for $n \geq 3$.

$$\frac{\sigma_{\theta\theta}}{\sigma_0} = \left(\frac{J}{\alpha\varepsilon_0\sigma_0 I_n L}\right)^{\frac{1}{n+1}}\left[\left(\frac{r}{L}\right)^{s_1}\tilde{\sigma}_{\theta\theta}^{(1)}(\theta) + A_2\left(\frac{r}{L}\right)^{s_2}\tilde{\sigma}_{\theta\theta}^{(2)}(\theta) + (A_2)^2\left(\frac{r}{L}\right)^{s_3}\tilde{\sigma}_{\theta\theta}^{(3)}(\theta)\right] \quad (1)$$

Therefore, using the RKR [11] critical stress fracture criterion, when the critical stress is at a *finite r* from the crack tip, it is logical to postulate that the fracture initiation is controlled by these two parameters. It is worth noting that, at this moment, both J and A_2 are merely two mathematical coefficients resulted from solving the nonlinear homogeneous partial differential equations. They had no real "physical" meaning until later, through an energy argument like Rice first showed that the coefficient J is path independent [7] and the testing procedure was developed by Landes and Begley [12,13] to *measure* the critical J-value and "designated" it as the fracture toughness of the material. As for the second mathematical coefficient A_2, *since it is a function of specimen/structure geometry and loading level,* naturally it can be adopted as a quantitative measure of the geometry effect and, therefore, the "constraint effect."

In the past decade, the J-A_2 methodology using Eq. (1) has been applied to the interpretation of fracture initiation [14, 15], ductile crack growth [16,17], and dynamic fracture [18]. Specimen size requirement for a two-parameter fracture toughness testing procedure is proposed in [19, 20] which shows a much relaxed specimen size requirement compared with the stringent requirement in ASTM single-parameter testing procedure. Furthermore, the distinct crack tip fields in low hardening material for various specimens [3] can now be explained by adding terms with the constraint parameter. For example, the Prandtl or slip line field in the CCP specimen can be generated by varying the value of the constraint [21].

Note that other methodologies were also proposed for quantifying the constraint effect in fracture, such as the J-Q and J-T theories [1,2]. Interested readers may easily find the references in open literature.

3. Constraint effect in fracture of linear materials [22-24]

For brittle materials, the crack tip fields may be represented by the Williams series solution from linear elasticity theory [25] as

$$\sigma_{ij} = \sum_{n=1}^{\infty} B_n r^{\frac{n}{2}-1} f_{ij}^{(n)}(\theta) \quad (2)$$

Note that B_n are the undetermined mathematical coefficients which came from solving the linear homogeneous differential equations. If a fracture event is controlled by the opening stress within a process zone (or at a critical distance) in which the first term dominates and, furthermore, if the RKR model is adopted, then

$$\sigma_C = \frac{K_C}{\sqrt{2\pi r_C}} \quad (3)$$

The subscript "C" denotes critical and $\frac{K}{\sqrt{2\pi}} = B_1$. The traditional single parameter "fracture criterion", $Kc > K_{IC}$ is therefore equivalent to the RKR model, that is, "a critical stress σ_c is attained at a critical distance r_c ahead of the crack tip" (see Eq. (3)). It relates the mathematical coefficient B_1 in Eq.(2) to the crack growth resistance (or fracture toughness) of the material (K_{IC}) [26].

If the fracture event is controlled by stress/strain at a *finite* distance r from the crack tip such as that shown in Figure 1, then the "traditional fracture criterion," Eq.(3), may not be sufficient. For example, Figure 3 shows the opening stress in front of a crack tip in four cases, SE(T), SE(B), shallow (a/W=0.05) and deep crack (a/W=0.5). As shown in Figure 3, as r comes close to zero, all four cases approach to the K-field, which is the leading term in Eq. (2) when small strain formulation is used. At a finite r, the two shallow (deep) cracked specimens have stresses higher (lower) than the K-field. The difference between the actual stress and the K-field is from the higher order terms in Eq.(2).

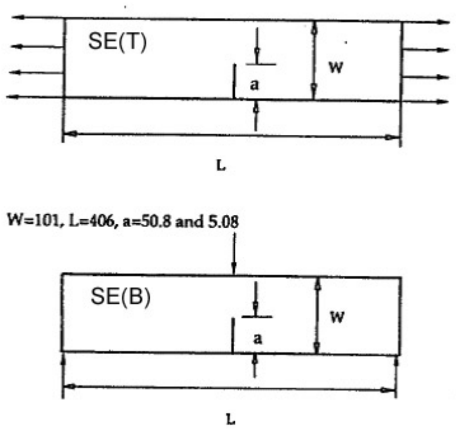

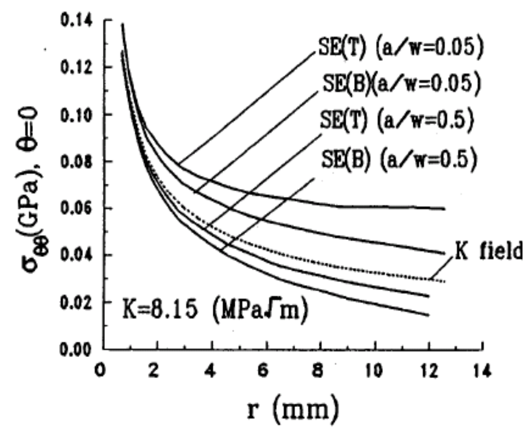

Figure 3 Crack opening stresses in SE(B) and SE(T) with shallow (a/W=0.05) and deep (a/W=0.5) cracks

The real question is "how large is the critical distance r_c where the critical stress resides?" If it is sufficiently small, for example, r_c approaches zero, then a single parameter K can be used to determine the fracture event with Eq. 3. If, however, r_c is relatively large such that at $r = r_c$ the stress field deviates significantly from the K-field, then the higher order terms must be considered to accurately quantify the actual stress state and, consequently, to characterize the fracture event.

Applying the RKR fracture model and keeping two terms in Williams solution (Eq. 2), it can be shown that

$$\sigma_C = \frac{K_C}{\sqrt{2\pi r_C}} + 3B_C\sqrt{r_C} \tag{4}$$

Note that the second term in Eq. 2 containing the T-stress (a constant stress parallel to the crack face) vanishes at $\theta = 0$. Instead, the third term in Eq. 2 is used in Eq. 4 as the additional term. If, on the other hand, one adopts a critical strain fracture criterion and solves for the opening strain along $\theta = 0$, one would have

$$\varepsilon_c = \frac{(1+\upsilon)(1-2\upsilon)}{\mathrm{E}}\frac{K_C}{\sqrt{2\pi\,\mathrm{r_c}}} - \frac{(1+\upsilon)\upsilon}{\mathrm{E}}\mathrm{T_c} \qquad \text{for plane strain case} \tag{5}$$

Equations 4 and 5 indicate that the critical stress intensity factor or the apparent fracture toughness K_c of a material increases with the T-stress (Eq. 5) or the negative of A_3 (Eq. 4). This trend is summarized in Figure 4.

Note that when the second term in either Eq. 4 or 5 becomes significantly large the maximum opening stress/strain is no longer ahead of the crack tip along the $\theta = 0$ direction even under pure Mode I conditions. Crack curving would then take place based on a maximum opening stress fracture criterion. It has been shown that the fracture toughness reduces when curving occurs (Fig. 4).

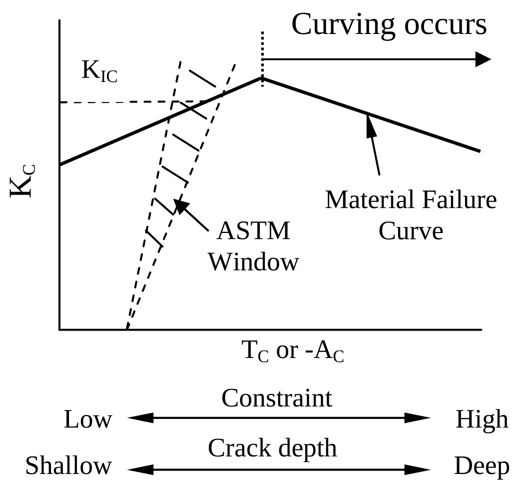

Figure 4 Variation of apparent fracture toughness with constraint, crack curving, and its relationship with the ASTM window

Furthermore, it appears that using different ASTM recommended specimen geometries for fracture toughness testing (e.g., three-point bend and compact tension specimens) would create an "ASTM window" as plotted in Figure 4. This is caused by the range of T or A_3 values inherently to various standard ASTM specimens. As a result, the K_{IC} determined by applying the ASTM testing procedure is a subset of the complete K_C curve (or the "material failure curve"). It is clear from Figure 4 that K_{IC} determined inside the ASTM (e.g. E 399) window is conservative when used for structure integrity assessment for specimens/structures with smaller A_3 or greater T (i.e., higher constraint configuration) but *not* conservative otherwise. A direct impact of this would be in structures having biaxial stress fields such as pressure vessels and piping in which the T-stress would indeed play an important role in fracture.

4. Comparison of the constraint effect in fracture in elastic and elastic-plastic materials

As outlined in the previous sections, the "constraint effect" in fracture could occur in either linear elastic or elastic-plastic materials. The fundamental reason to have the constraint effect is the deviation of the stress state from the asymptotic HRR solution (or K-solution) in elastic-plastic (or elastic) materials.

Categorically, fracture mechanics community classifies the shallowly cracked or tension specimen as low constraint; and the deeply cracked or bending specimens as high constraint. This is based on the classical concept or "contained plasticity" as discussed in section 1. For elastic-plastic materials, low constraint specimen or structure would have higher fracture toughness (as the stress is lower than the HRR stress, see Fig. 1). The material failure curve is schematically shown in Figure 5.

Comparing the material failure curves in Figures 4 and 5, a very interesting observation can be made, that is, the effect of constraint on failure in these two materials (linear elastic and elastic-plastic) is entirely opposite. In the linear elastic case, lower fracture toughness can be obtained from low constraint specimens. This can be explained from Figure 3, in which the shallow cracks (i.e. low constraint specimens) in fact have stresses higher than the *K*-stress.

The knowledge of material failure mode as either brittle (limited plasticity) or ductile (substantial plastic deformation) is therefore extremely important when applying the constraint theory to the structural integrity assessment. Not only the underlying fracture mechanics theories for the two materials are different, but also the resulting fracture toughness could be completely dissimilar.

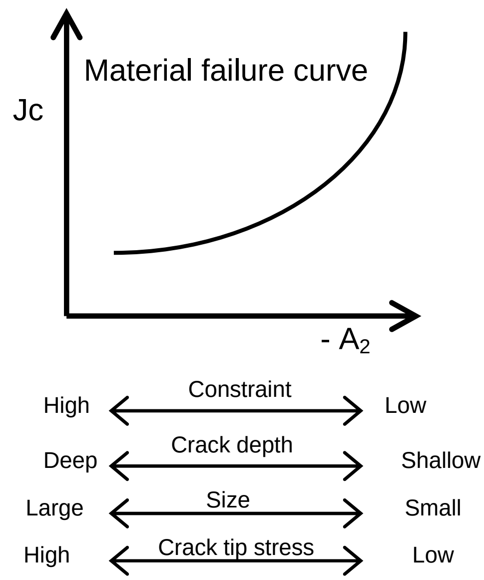

Figure 5 Material's failure curve in elastic-plastic material and its relationship with the constraint

5. Acknowledgement

Fracture mechanics research at the University of South Carolina has primarily been sponsored by NSF and Savannah River National Laboratory. The authors also would like to thank all former graduate students, post-doctors and visiting researchers (e.g., Drs. Xian-Kui Zhu, Yil Kim, Shu Liu, and Shaouri Yang). The results summarized in this paper would not be possible without their diligent work.

6. References

[1] E. M. Hackett, K.-H. Schwalbe, and R.H. Dodds, Jr., Editors, Constraint Effects in Fracture, *ASTM STP 1171,* American Society for Testing and Materials, West Conshohocken, 1993.

[2] M. Kirk and A. Bakker, Editors, Constraint Effects in Fracture – Theory and Applications: second Volume, *ASTM STP 1244*, American Society for Testing and Materials, West Conshohocken, 1994.

[3] F. A. McClintock, Plasticity aspects of fracture, in Fracture: An Advanced Treatise, Vol.3, H. Liebowitz (Ed.), Academic Press, New York, (1971) 47-225.

[4] J. W. Hutchinson, Singular behavior at the end of a tensile crack in a hardening material, J. Mech. Phys. Solids, 16 (1968) 13-31.

[5] J. W. Hutchinson, Plastic stress and strain fields at a crack tip. J. Mech. Phys. Solids, 16 (1968) 337-347.

[6] J. R. Rice and G. F. Rosengren, Plane strain deformation near a crack tip in a power law hardening material. J. Mech. Phys. Solids 16 (1968) 1-12.

[7] J. R. Rice, A path independent integral and the approximate analysis of strain concentration by notches and cracks. J. Appl. Mech. 35 (1968) 379-386.
[8] S. Yang, Y. J. Chao, and M. A. Sutton, Complete theoretical analysis for higher order asymptotic terms and the HRR zone at a crack tip for Mode I and Mode II loading of a hardening materials, Acta Mechanica, 98 (1993) 79-98.
[9] S. Yang, Y. J. Chao, and M. A. Sutton, Higher order asymptotic crack tip fields in a power-law hardening material, Engineering Fracture Mechanics, 45(1) (1993)1-20.
[10] Y. J. Chao, S. Yang, and M. A. Sutton, On the fracture of solids characterized by one or two parameters: theory and practice, Journal of Mechanics and Physics of Solids, 42(4) (1994) 629-647.
[11] R.O. Ritchie, J.F. Knott, and J.R. Rice, On the relationship between critical tensile stress and fracture toughness in mild steel, Journal of the Mechanics and Physics of Solids, 21 (1973) 395-410.
[12] J. D. Landes and J. A. Begley, The J integral as a fracture criterion, Fracture Toughness, *ASTM-STP-514*, 1-20, American Society for Testing Materials, Philadelphia. PA. 1972.
[13] J. D. Landes and J. A. Begley, Test results from J integral studies: an attempt to establish a J_{Ic} testing procedure, Fracture Analysis, *ASTM-STP-560, 170-186,* American Society for Testing Materials, Philadelphia, PA, 1974.
[14] Y.J. Chao and P.S. Lam, Effects of crack depth, specimen size, and out-of-plane stress on the fracture toughness of reactor vessel steels, ASME Journal of Pressure Vessel Technology, 118 (1996) 415-423.
[15] Zong-An Chen, Zeng Zhen, and Yuh J. Chao, Effect of crack depth on the shift of the ductile-brittle transition curve of steels, Engineering Fracture Mechanics, 74 (2007) 2437-2448.
[16] Y. J. Chao and X. K. Zhu, Constraint-modified J-R curves and Its application to ductile crack growth, International Journal of Fracture, 106(2) (2000)135-160.
[17] P. S. Lam, Y. J. Chao, X. K. Zhu, Y. Kim, and R. L. Sindelar, Determination of constraint-modified J-R curves for carbon steel storage tanks, ASME Journal of Pressure Vessel Technology, 125 (2003) 136-143.
[18] Y. Kim and Y.J. Chao, Effect of loading rate on dynamic fracture initiation toughness of brittle materials, International Journal of Fracture, 145 (2007) 195-204.
[19] Y. J. Chao, and X. K. Zhu, J-A_2 characterization of crack-tip fields: extent of J-A_2 dominance and size requirements, International Journal of Fracture, 89(3) (1998) 285-307.
[20] Y. J. Chao, and X. K. Zhu, Specimen size requirement for two-parameter fracture toughness testing, International Journal of Fracture, 135 (2005) 117-136.

[21] X. K. Zhu and Y. J. Chao, Constraint effects on crack tip fields in elastic-plastic materials under Mode-I, II or mixed Mode I/II loading, Journal of the Mechanics and Physics of Solids, 49(2) (2001) 363-399.
[22] Y. J. Chao, S. Liu and B. Broviak, Brittle fracture: constraint effect and crack curving under Mode I conditions, Experimental Mechanics, 41(3) (2001) 232-241.
[23] Y. J. Chao, and X. Zhang, Constraint effect in brittle fracture, 27th *National Symposium on Fatigue and Fracture, ASTM STP 1296,* R. S. Piascik, J. C. Newman, Jr., and D. E. Dowling, Eds., American Society for Testing and Materials, West Conshohocken, 1996.
[24] S. Liu and Y.J. Chao, Variation of fracture toughness with constraint, International Journal of Fracture, 124 (3-4) (2003) 113-117.
[25] M. L. Williams, On the stress distribution at the base of a stationary crack, ASME Journal of Applied Mechanics, 24 (1957) 109-114.
[26] G. R. Irwin, Plastic zone near a crack and fracture toughness, Mechanical and Metallurgical behavior of sheet materials, Proceedings Seventh Sagamore Ordinance Materials Conference, (1960) IV-63-IV-78.